Chapter 5

Heat transfer coefficient and productivity of the frugal solar still integrated with a novel economic model

5.1 Overview

An experimental study has been conducted during summer season of our country (May-June) using our solar still with copper cylinders filled with paraffin wax (PCM) and doped by nanoparticles to observe the drastic improvement in solar distillate due to higher solar intensity. After establishing the proof of concept of our novel frugal solar still, the price of the distilled water has also been estimated which is sufficiently lower as compared to the traditional distilled water due to its technological advantage. Further, an economic model has also been developed for the market entry of our proposed solar still under duopoly scenario. It has also been observed that after a certain threshold our product will enjoy better market share rather than the traditional one which justifies the deployment of our solar still in resource constrained settings for further commercialization.

5.2 Materials and methods

5.2.1 Experimental part

Schematic of experimental setup is shown in Fig. 5.1. A single slope solar still is fabricated and used to conduct the experimental part of the present work. The solar still is made of a square stainless steel basin covered with a 4 mm thick condensing glass panel with a slope of 32°. At the bottom side of the still basin, six copper cylinders, placed with paraffin wax (PCM) doped with CuO (nanoparticle), are laid down and fully submerged under the water. The copper cylinders are constructed with 7 cm diameter and 7 cm height, have been sealed with rubber rings operational within the desired range of temperature in the present study. Fig. 5.2 shows the actual pictorial view of the solar still unit. The solar still basin had a square shape of 75 cm

length and 75 cm of width, while its height from the front side is 15 cm as shown in Fig. 5.1. The cover is substantially transparent to solar radiation and opaque to infrared and serves as a condenser for the saturated vapor within the solar still.
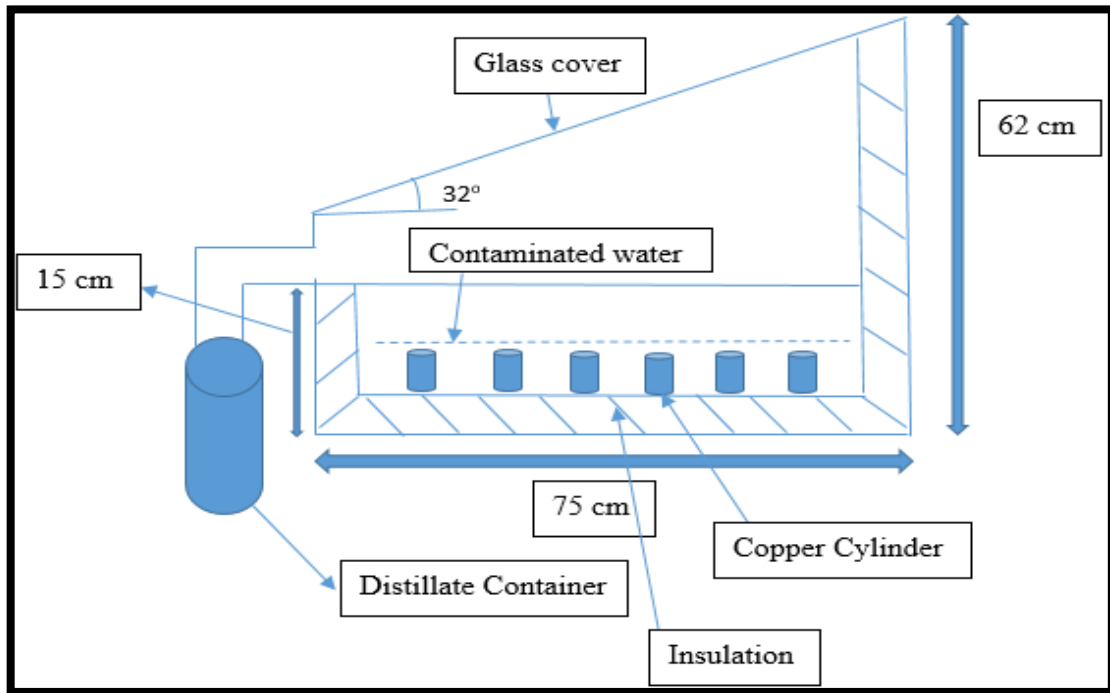

Fig. 5.1 Schematic diagram of single slope solar still integrated with absorbing materials
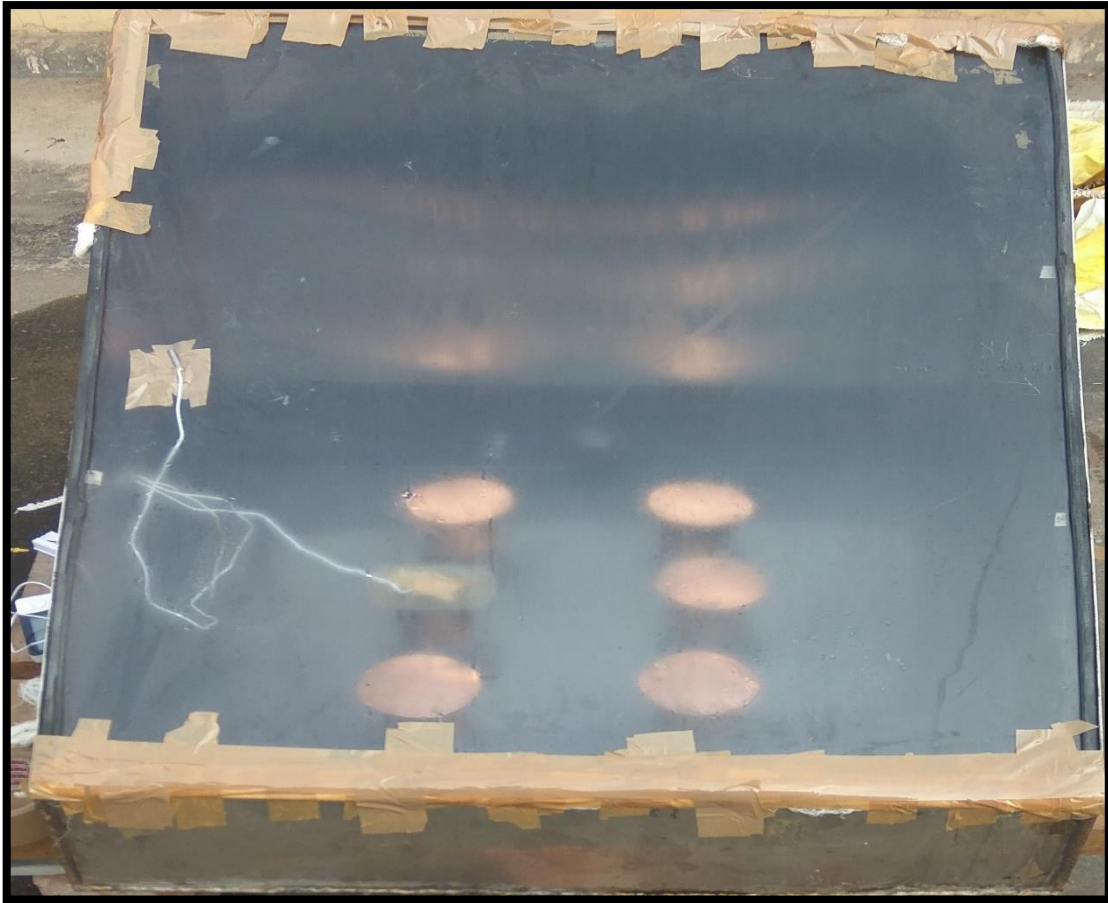
Fig. 5.2 Experimental setup of single slope solar still

The radiation shape factor strongly depends on the solar still geometry especially the portion of the inclined glass cover with respect to the basin water at the horizontal level, although the distillation output varies very little with the variation of the inclination of the glass cover. In the present study, the quantity of water level in the basin has been kept around 7 cm.

The thermo-physical properties of energy absorbing materials and nanoparticle specifications are given in Tables 5.1 and 5.2 respectively. Table 5.3 and Table 5.4 provide the values of experimental variables as well as range and accuracy of each measuring instruments which have been used in this present work.
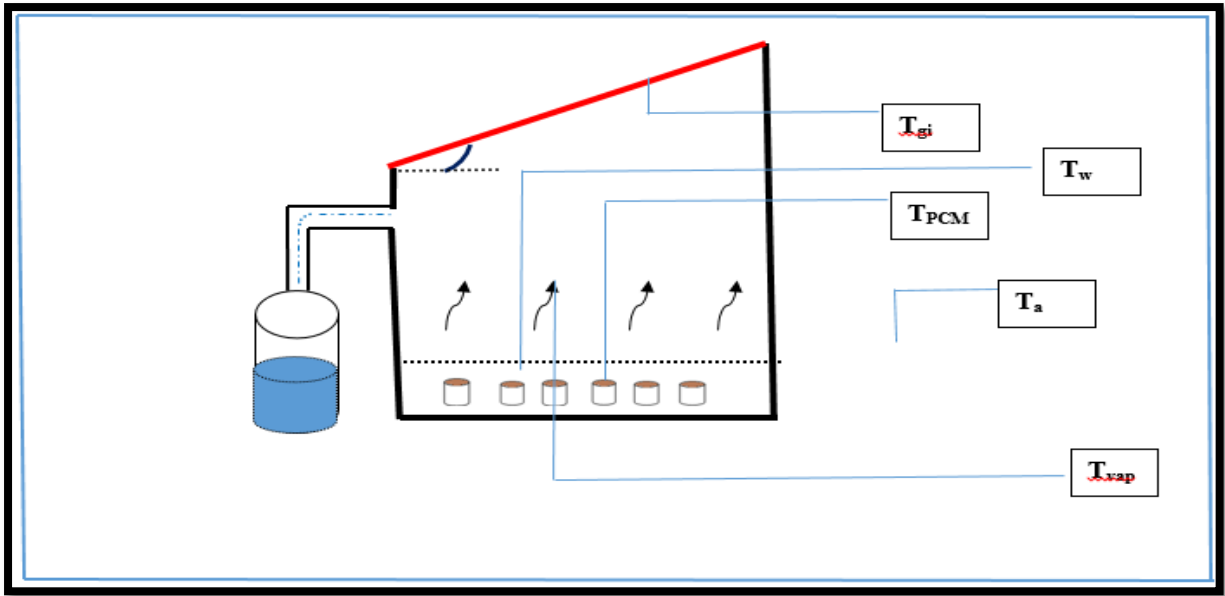
Fig. 5.3 Locations of thermometer sensors in the experimental setup

Table 5.1 The properties (thermo-physical) of paraffin wax (Farid et al., 2004; Sharma et al.,

2009; Zalba et al., 2003)

Thermo-physical properties	Paraffin wax
Chemical formula	($C_{31}H_{64}$)
Melting point (ºC)	58-60ºC
Latent heat (fusion), kJ/kg	226
Density (solid), kg/m^3	818
Conductivity (thermal), W/m-K	0.25
Specific heat, kJ/kg-ºC	2.95

Table 5.2 The used nanoparticle (CuO) specifications

Item	CuO specifications
Manufacturer	Sisco research laboratories pvt. Ltd. (28954)
Assay	Min. 99%
Appearance	Black powder
pH value	7.5
Grain size (nm)	40
Thermal conductivity, W/m-K	0.34

Table 5.3 Experimental variables

Variables	Symbols	Value
Transmittance (glass cover)	τ_g	90%
Absorptivity (glass cover)	ε_g	5%
Wind speed	V	1 m/s
Density (water)	ρ	989 kg/m^3
Latent heat of vaporization	h_{fg}	2372 (KJ/kg)
Declination angle	δ	32º
Latitude of Varanasi	φ	25.31º

Table 5.4 Range of various instruments with their accuracy

S. No.	Instruments	Accuracy	Range
1	Solar power meter	10 W/m^2	0 - 1999 W/m^2
2	Thermocouple (PT-100)	$\pm$ 1°C	-50 - 110°C
3	Measuring cylinder	$\pm$ 10 ml	0-2000 ml
4	Anemometer	1-4	0.4-30 m/s
5	Hygrometer (Ambient temperature)	$\pm$ 1°C	-50 - 70°C

The experiments were carried out during summer from May to June, 2020 in Indian Institute of Technology, Department of Mechanical Engineering, Banaras Hindu University, India. The experiments were started from at about 9 am and finished at about 9 pm, and the weather during the experimentation was clear. The experimental variables such as glass cover, ambient, PCM, NPCM and basin water temperature have been measured hourly. The temperatures at different points have been recorded using P-T 100 thermometer.

5.2.2 Data collection

In the present work, a thermometer (P-T 100) has been used to measure different temperatures during each experiment. Fig. 5.3 shows a schematic diagram of the thermometer locations to record temperature readings hourly. Thermometer sensors have been connected inside the solar still system to measures basin water temperature (T_w), temperature of glass cover inner surface (T_{gi}), temperature of PCM (T_{PCM}), and outside to record ambient temperature (T_a). This kind

of thermometers has good specification and has been used for the measurement of temperature ranges within solar still system.

5.2.3 Impact of nanoparticle in the productivity of single slope solar still

Naveenkumar et al. (Naveenkumar et al., 2020) examined the impact of adding nanoparticles in single slope solar still numerically. The distillate of solar still was improved 60% to 90% when utilizing CuO and Al_2O_3 nanoparticles with passive and active solar stills. Chaichan et al.(Chaichan and Kazem, 2018) analysed the effect of adding alumina nanoparticle in paraffin wax and suggested that the properties such as thermal conductivity and stability are significantly increased. Zanganeh et al.(Zanganeh et al., 2019) examined that the impact of applying materials with various wettability on the condensing surface towards the yield of solar still. In this study, nano-silicon material was applied on the condensing surface to compare the impact of film wise and drop wise condensation towards the productivity of solar still. The results showed that using of nanomaterial altered the condensation process to drop wise from film wise for all the materials. Parsa et al. (Parsa et al., 2020) experimentally examined that the three different modified simple single slope solar stills with thermoelectric heating, thermoelectric heating integrated with silver nanofluid and thermo electric heating integrated with silver nanofluid as well as external condenser. The results indicate that the silver nanofluid integrated with external condenser produces the maximum cumulative production of 7760 $cc/m^2/day$. The results also indicate that the addition of condenser in the solar still raises the production rate by 26.30%.

5.2.4 Thermal analysis

The frugal design has been emergent for an inside black painted basin area to dope copper oxide nanoparticles (CuO) and paraffin wax in order to reduce heat losses inside the solar still basin. For a solar still, solar radiation plays crucial role to enhance the heat transfer inside the basin. The solar radiation is absorbed by condensing cover and transmitted through the

absorbing materials, copper oxide and paraffin wax. The energy equilibrium equation has been constructed for single slope single basin solar still following the assumptions as mentioned below:

- Single slope solar still should be full tight during the experimental work.

- The energy storage materials have been kept in a completely insulated structure of solar still and heat transfer through the glass cover of the solar still has been considered negligible.

- Heat transfer inside the stored copper cylinders and paraffin wax is predominantly due to conduction. However, convection does not occur in copper cylinders when paraffin wax is melted.

- In this work, thermal gradient is not considered throughout the experimental procedure, and its average temperature values have been proposed for all calculations of heat transfer calculations.

The evaporative, radiative and convective heat transfer coefficients were calculated using the following equations of Dunkle (Dunkle, 1961) and Copper (Cooper and Read, 1974). At a given temperature inside the solar still evaporation occurs when the water vapour pressure becomes lower than that of its saturation pressure. The evaporative mode of heat transfer occurs between the water liquid-vapour interfaces and can be expressed as in Eq. (5.1):

$$Q_{ewg} = h_{ewg} \times (T_w - T_{gi}) \tag{5.1}$$

,where h_{ewg} has been calculated by using Dunkle (Dunkle, 1961) correlation as given in Eq. (5.2):

$$h_{ewg} = 0.016273 \times h_{Cwg} \times \left[\frac{P_w - P_{gi}}{T_w - T_{gi}}\right] \tag{5.2}$$

The radiative heat transfer rate between the glass cover surface, and water can be calculated using Eq. (5.3) and, h_{rwg} has been calculated using Eq. (5.4):

$$Q_{rwg} = h_{rwg} \times (T_w - T_{gi}) \tag{5.3}$$

$$h_{rwg} = \varepsilon_{eff}\sigma \left[(T_w + 273)^2 + (T_{gi} + 273)^2 \right] (T_w + T_{gi} + 546) \tag{5.4}$$

The convective heat transfer between the glass cover and water basin surface occurred through the humid air and existed because of the temperature difference between them. Inside the solar still, the convective rate of heat transfer can be determined using Eq. (5.5):

$$Q_{Cwg} = h_{Cwg} \times (T_w - T_{gi}) \tag{5.5}$$

,where h_{cwg} is the convective heat transfer coefficient from water to inner surface of the glass cover. It has been calculated using Eq. (5.6):

$$h_{Cwg} = 0.884 \left\{ (T_w - T_{gi}) + \frac{[P_w - P_{gi}][T_w + 273.15]}{[268900 - P_w]} \right\}^{\frac{1}{3}} \tag{5.6}$$

5.3 Results and discussion

5.3.1 Hourly variation of solar intensity, ambient and glass cover temperature

In this work, several experiments have been conducted during May to June 2020 in Varanasi, India. Fig. 5.4 shows the hourly variation of solar intensity and ambient temperature in all three conditions. Beyond the sunshine hours, solar intensity becomes almost zero which has been depicted in Fig. 5.4 after 18 hour. It also shows that solar intensity in India is very high (about 950 W/m^2) in the month of June, which is considered as the peak of summer season. Even though for all three cases, the experiments have been performed on three different days, the variation in solar intensity and ambient temperature have been nominal, suggesting that the

performance of the solar still would not have been interfered due to minor variations of meteorological parameters.

Fig. 5.5 represents the hourly variation of glass cover temperature for SSS, SSPCM, and SSNPCM. It is observed that the variation of glass cover temperature for three conditions has been the same and close to each other as compared to that of the water basin. The similar glass cover temperature for all three conditions have been due to high transmittance (95%) and lower absorptivity (5%) of glass. The temperature of glass increased with time and reached the highest temperature during 1 – 2 pm. It can also be considered that the temperature of the inner glass has been close to the temperature of the water during the early hours of the day. However, as the time of sunshine increases, the difference between glass and water widens due to water absorbing some of the incident solar radiation and also, receives heat from the basin liner, while the transparent glass cover transmits maximum incident solar radiation.
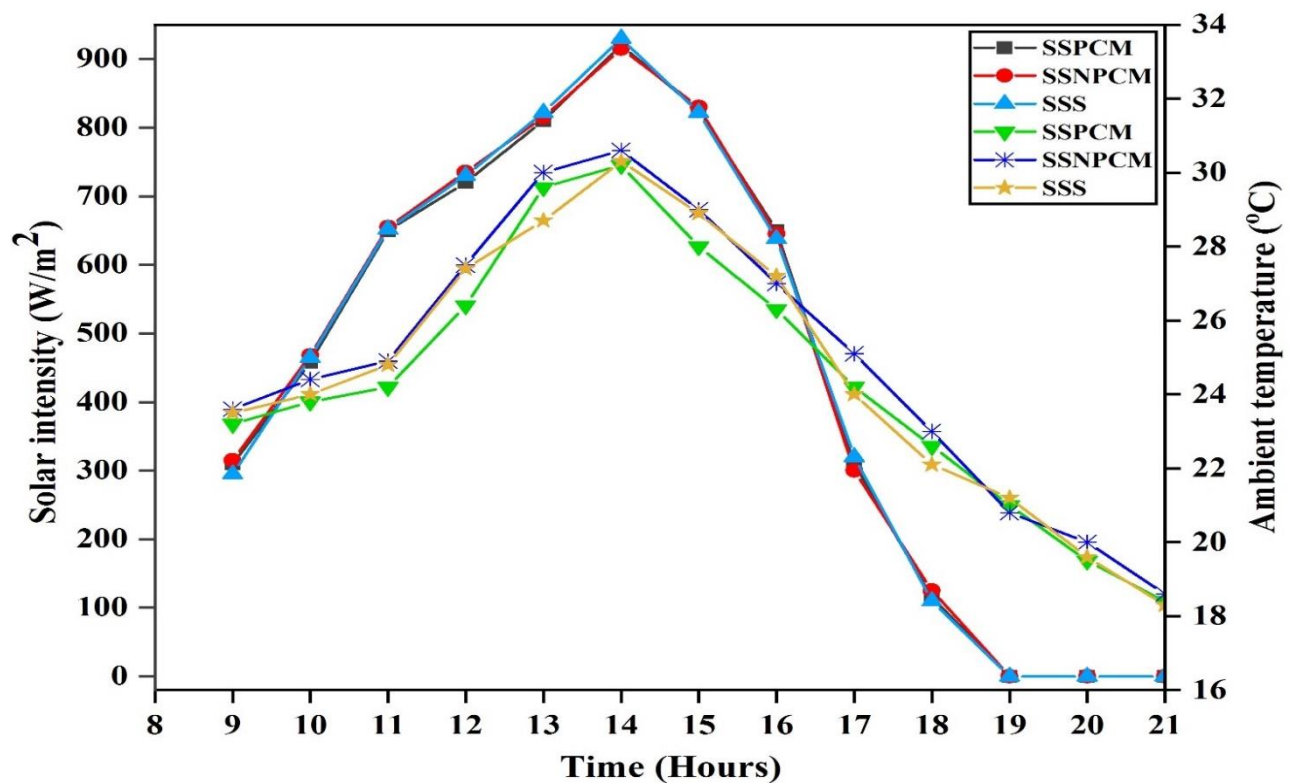

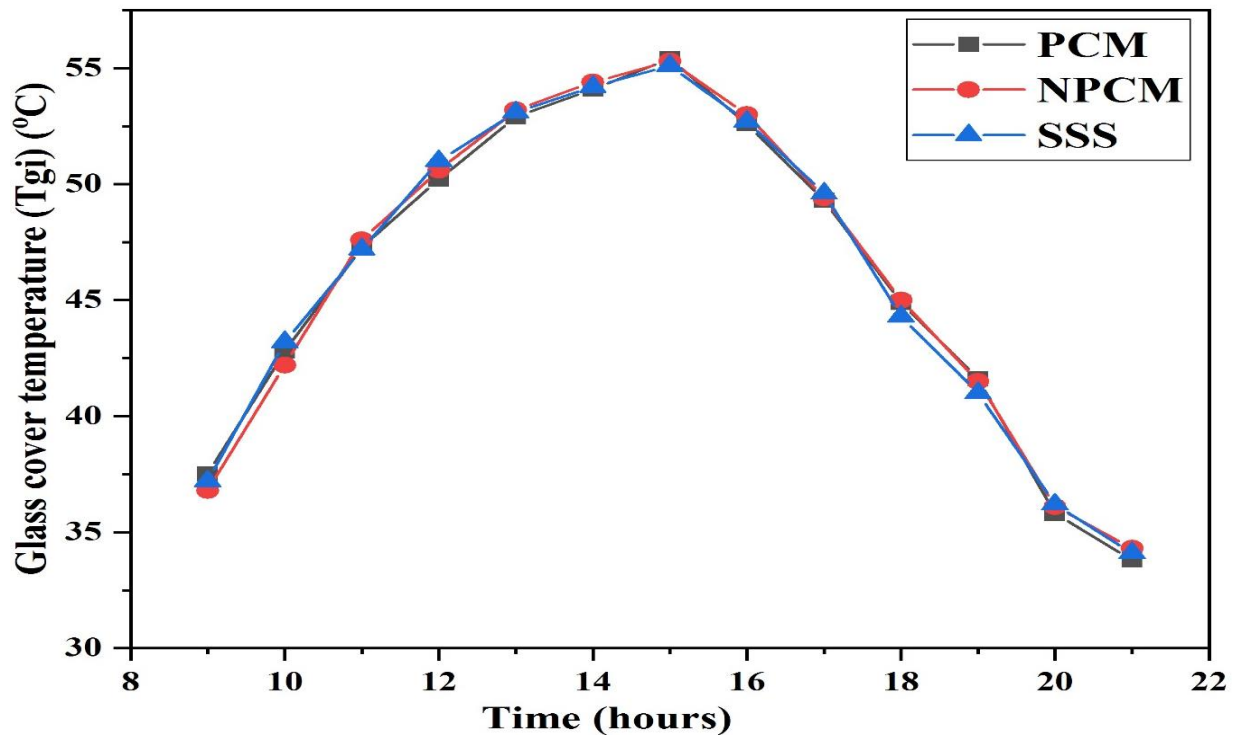**Fig. 5.4** Hourly variation of solar intensity and ambient temperature

Fig. 5.5 Hourly variation of glass cover temperature

5.3.2 Variation of heat transfer coefficient for SSS, SSPCM, and SSNPCM

Figs. 5.6-5.9 indicate the hourly variation of heat transfer coefficients (h_{ewg}, h_{rwg}, h_{cwg} and h_t) associated with the single slope solar still units. In the present study, the calculation of the heat transfer coefficients associated with water and glass cover is necessary because maximum heat loss occurs between these two components during charging and discharging mode. In the observed period, the evaporative heat transfer coefficient plays a major role in total heat transfer between the water basin and glass cover as compared to radiative and conductive heat transfer coefficients. The maximum value for h_{ewg} (SSNPCM=33.45, SSPCM=32.97, and SSS=33.98 W/m²-K), h_{rwg} (SSNPCM=4.94, SSPCM=4.97, and SSS=4.48 W/m²-K), h_{cwg} (SSNPCM=2.91, SSPCM=2.87, and SSS=2.59 W/m²-K), h_t (SSNPCM=40.80, SSPCM=40.23, and SSS=39.58 W/m²-K) have been found around 1-2 pm when the maximum temperature has been attained by the water basin.
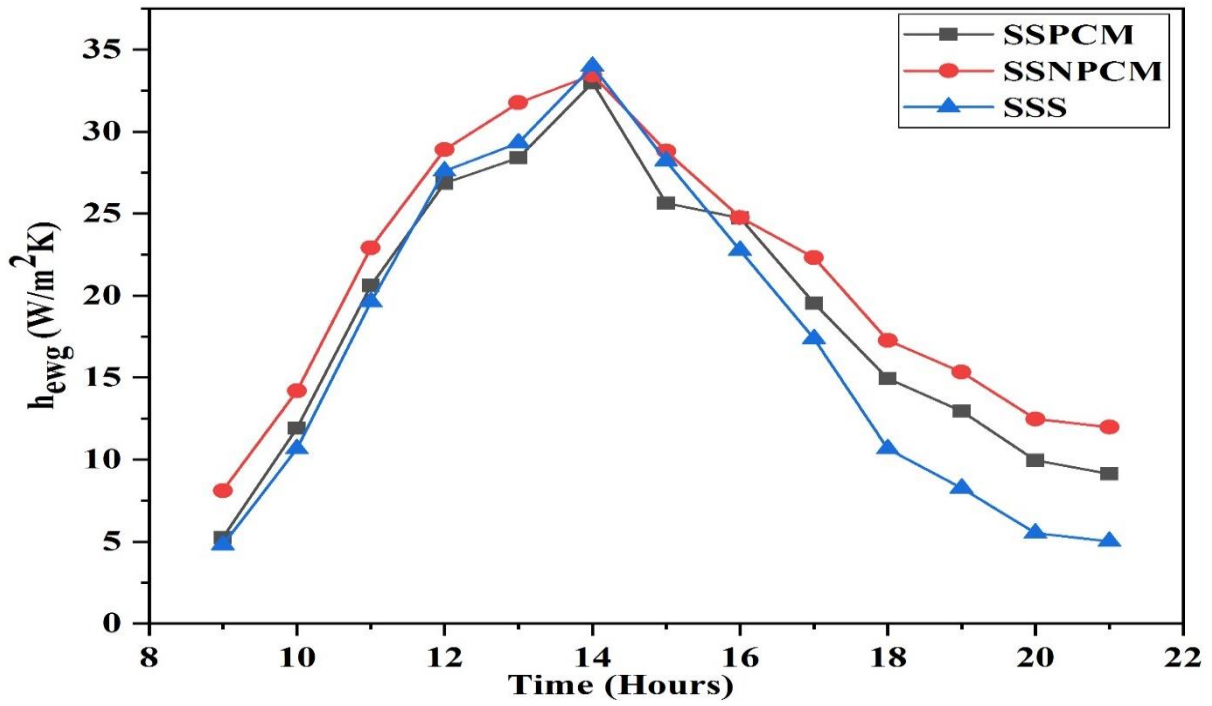
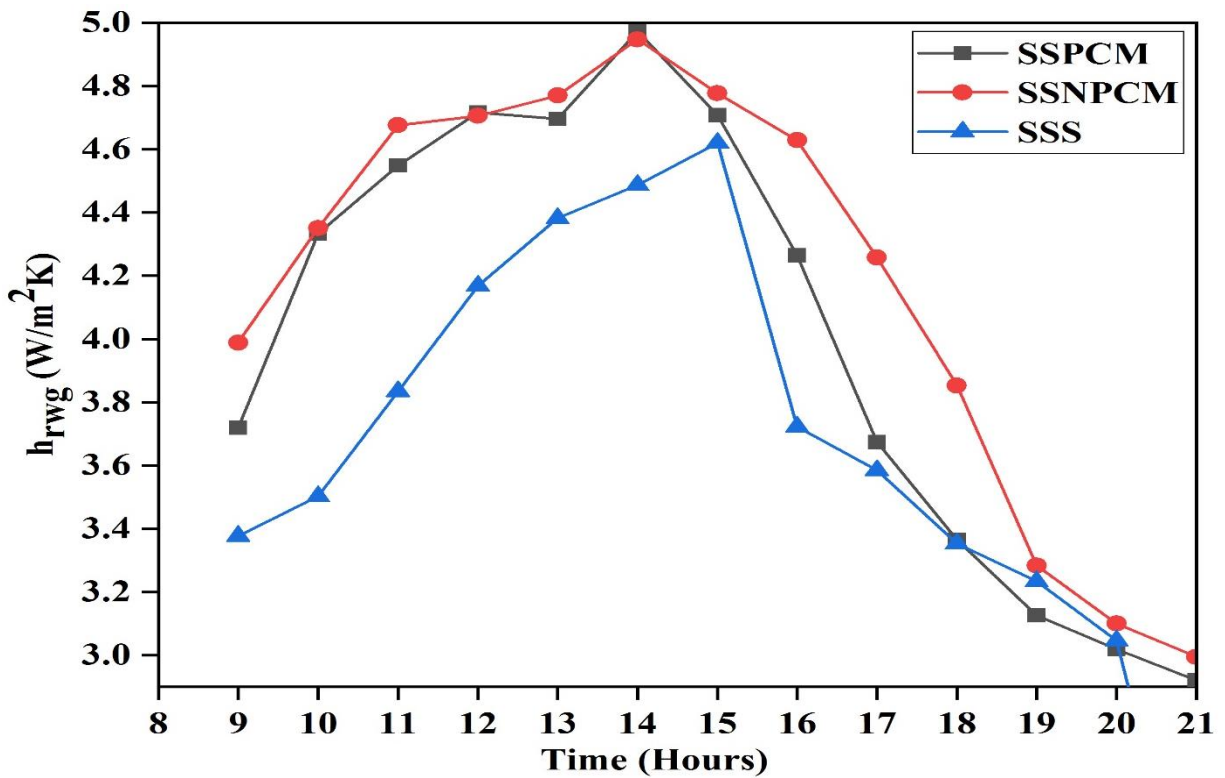**Fig. 5.6** Hourly variation of evaporative heat transfer coefficient

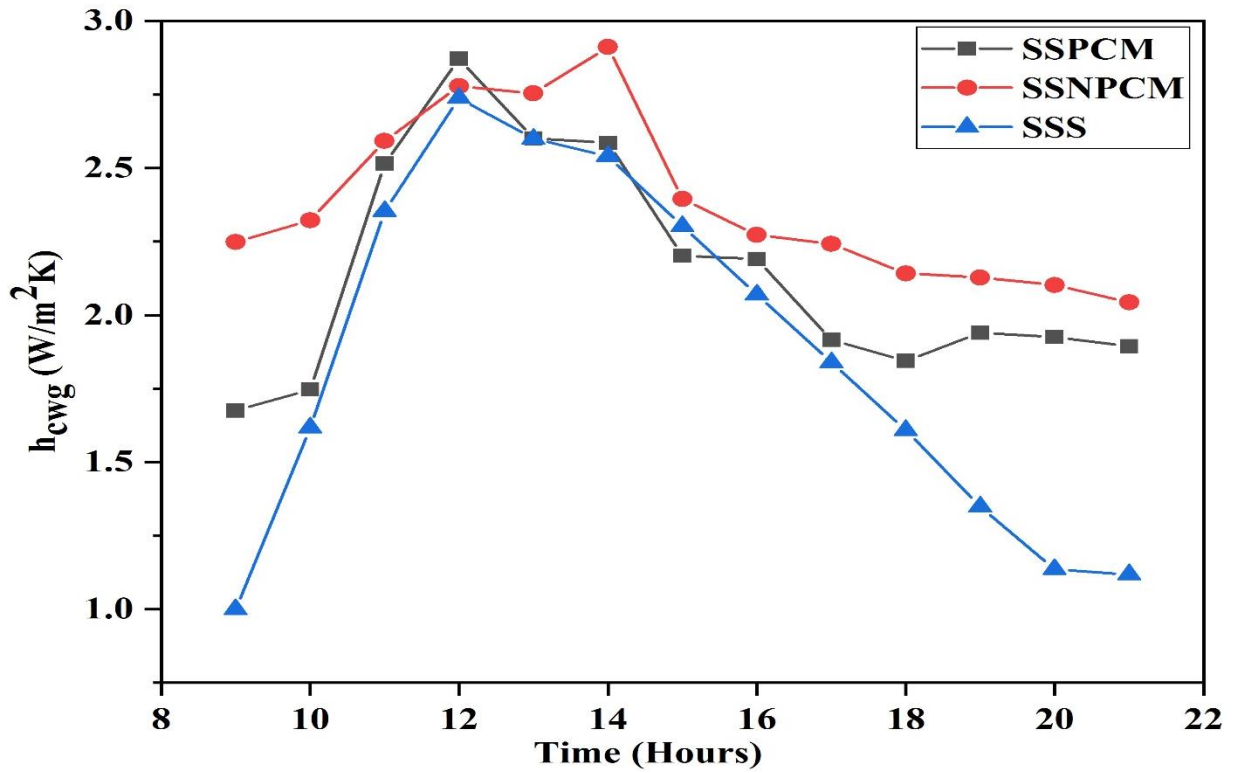**Fig. 5.7** Hourly variation of radiative heat transfer coefficient

Fig. 5.8 Hourly variation of convective heat transfer coefficient
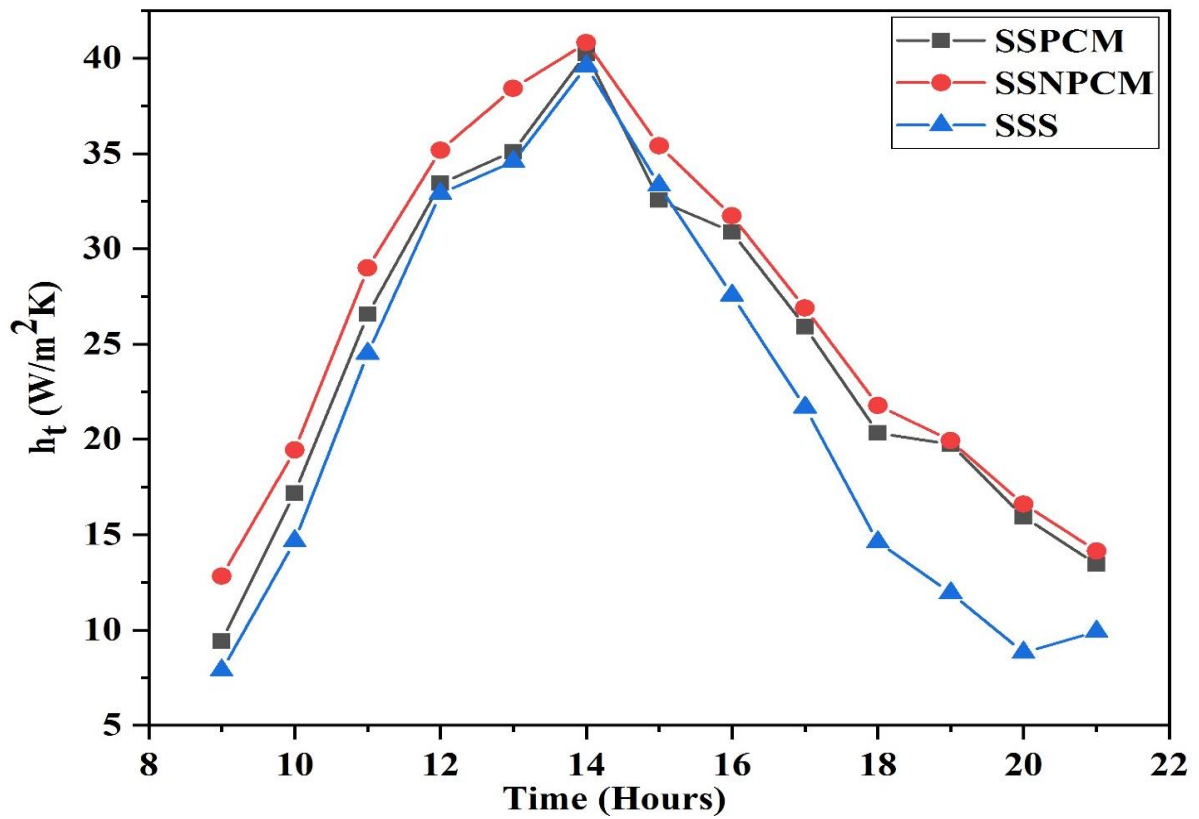

Fig. 5.9 Hourly variation of total heat transfer coefficient

The substantial-high values for the heat transfer coefficient associated with evaporative mode as compared to radiative and convective mode confirms the high rate of evaporation, resulting in distillate output. The rate of evaporative heat transfer depends greatly on the relative humidity and air-water temperature difference.
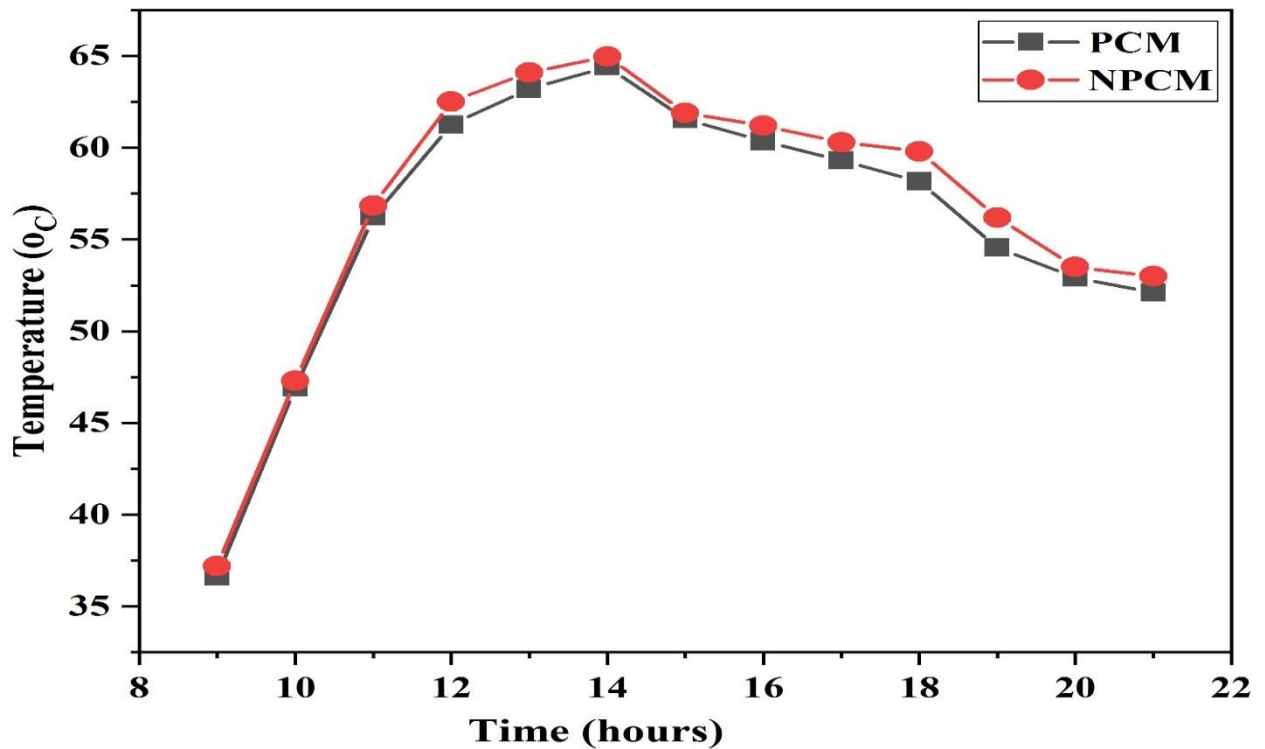

Fig. 5.10 Hourly variation of PCM and NPCM temperature

5.3.3 Hourly temperature variation of basin water, PCM, and NPCM

Fig. 5.10 represents the hourly variation of PCM and NPCM temperature. The basin has been coloured black so that it can absorb most of the incident radiation, and can transfer thermal energy quickly to the water basin. It has been observed that water temperature, glass temperature, PCM and NPCM temperature follow the same solar radiation intensity profile. As the solar radiation intensity increases with time, the rate of heat transfer increases due to convection from basin liner to water basin and further solar energy is stored in PCM and NPCM. Fig. 5.11 manifests the hourly variation of water basin temperature for all three cases (SSPCM, SSNPCM and SSS) and, it can be observed that the maximum temperature has been

recorded at 1-2 pm. The maximum temperature attained by SSNPCM (72.8 $^{\circ}$C) has been much higher as compared to SSS (68.23 $^{\circ}$C) and SSPCM (68.93 $^{\circ}$C), which results higher distillate output.
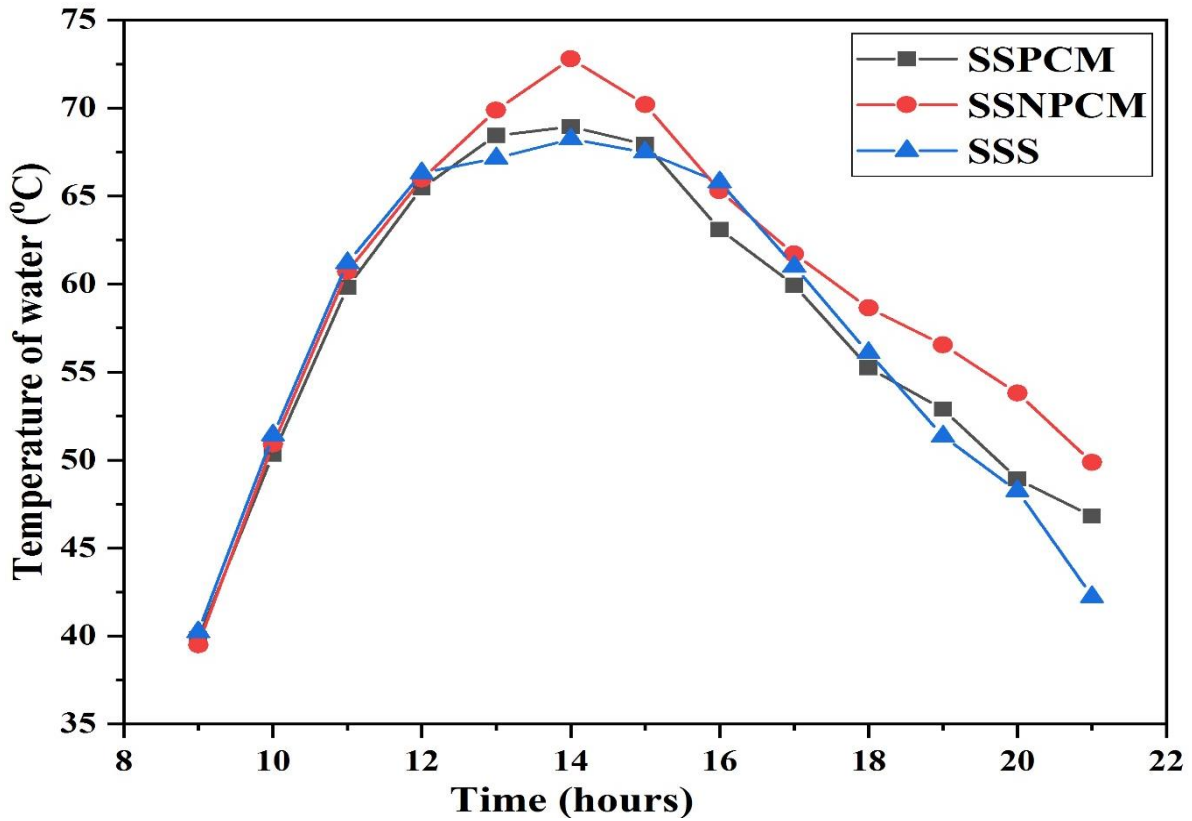

Fig. 5.11 Hourly variation of basin water temperature

In most of the operational hours, the water basin temperature of SSNPCM has been higher as compared to SSPCM and SSS due to the addition of nanoparticle, which increased the charging and discharging capacity of the system. The increase in the charging and discharging capacity of SSNPCM has been due to a significant increase in the thermal conductivity of the storage material.

The total daily distillate of SSS, SSPCM, and SSNPCM have been 2080, 2985, and 3970 ml/m^2-day. The total distillate for SSPCM has been increased significantly due to the introduction of PCM, which has led distillation to continue even in the absence of solar

radiation, while in the case of SSNPCM, the system has witnessed much higher output due to increased heat transfer rate by introducing nanoparticle in PCM.

5.4 Economic analysis of the proposed frugal solar still with PCM and nanoparticle

It is important to analyse the price of solar still considering nanoparticles integrated with paraffin wax as a novel approach to enhance distillation output. The present capital cost of the solar still is provided in Table 5.5.

The inputs to the calculation were present capital cost and capital recovery factor (CRF) which have been provided in Table 5.5. Numbers of years of operation (Y) and CRF are assumed to be 10 years and 0.177 respectively (Dsilva Winfred Rufuss et al., 2018; Kabeel et al., 2010; Yadav and Sudhakar, 2015). Using the inputs and assumptions, the outputs such as fixed annual cost (FAC), sinking fund factor (SFF), salvage value (S), average salvage value (ASV) and annual maintenance cost (AMC), annual cost (AC), average annual productivity (M) and cost per litre (CPL) associated with the solar stills for Indian climatic condition have been calculated using the following expressions and depicted in Table 5.6.

The unit cost of distilled water is the ratio of total annual cost of passive solar still per unit area and average annual productivity in liters of the solar still per unit area. It can be estimated using the following relation (Dsilva Winfred Rufuss et al., 2018).

$$CPL = \frac{AC}{M} \qquad (5.7)$$

,where total annual cost is of the passive solar still is calculated as:

$$AC = FAC + AMC - ASV \qquad (5.8)$$

Each factor of the Equation (5.8) is calculated by the relation given in the Equation (5.9), (5.10) and (5.11)

The fixed annual cost of solar still (FAC) is given as the product of the present capital cost (P) and capital recovery factory (CRF):

$$FAC = P \times CRF \tag{5.9}$$

,where the CRF is assumed to be 0.177 (Dsilva Winfred Rufuss et al., 2018).

And, annual maintenance cost (AMC) is assumed to be 15% of the fixed annual cost (FAC) as given in Table 5.5. Hence,

$$AMC = 0.15 \times FAC \tag{5.10}$$

Since annual salvage value (ASV) is the product of salvage value of solar still in future and sinking fund factor (SFF), it can be expressed as:

$$ASV = S \times SFF \tag{5.11}$$

,where the SFF and S can be calculate from Equation (5.12) and Equation (5.13):

$$SFF = \frac{i}{(i+1)^{y-1}} \tag{5.12}$$

$$S = 0.2 \times P \tag{5.13}$$

The average annual productivity in cost per liter (M) can be calculates as:

$$M = c \times n \tag{5.14}$$

,where 'c' is the distillate yield per day and 'n' is number of sunny days in a year, respectively. Which has been considered as 275 in our study (Ibrahim et al., 2015).

Table 5.5 The present capital cost of solar still units

Sl. No.	Materials	SSNPCM	SSPCM	SSS
1	Basin (stainless steel sheet)	5600	5600	5600
2	Fabrication cost	1500	1500	1500
3	Insulation	400	400	400
4	Glass cover	250	250	250
5	Absorbing coating	300	300	300
6	Copper cylinders (6 pieces)	2800	2800	-
7	PCMs	900	900	-
8	CuO nanoparticle	1500	-	-
9	Other cost	1000	1000	1000
	Total cost	**14250**	**9950**	**9050**

Table 5.6 Cost analysis of solar still units

Type of design	P	CRF	FAC	S	SFF	ASV	AMC	AC	M (L/Yr)	CPL (Rs.)
SSNPCM	14250	0.177	2522.25	2850	0.0432	123.12	378.33	2777.5	908	3.06
SSPCM	9950	0.177	1761	1990	0.0432	85.97	264.15	1939.18	621.5	3.12
SSS	9050	0.177	1601.85	1810	0.0432	78.19	240.28	1763.94	352	5.01

5.5 Payback period of solar still

The payback period is the minimum time required to recover investment costs involved for the

system. There are many methods for the estimation of it (Kabeel et al., 2010). For simplicity,

in the case of solar still, it is assumed that cash flow (CF) is the same for each year. Then, expression for the estimation of payback period can be expressed as:

$$\eta_p = \ln\left[\frac{CF}{CF-(P\times i)}\right] / \ln[1+i] \tag{5.15}$$

The payback period of solar still depends on overall cost of fabrication, maintenance cost, operating cost and cost of feed water (Ranjan and Kaushik, 2016). The cost of feed water may be consider as negligible. If the distillate produced by solar still is sold at market price (S_P), the CF can be calculated as:

$$CF = M \times S_P \tag{5.16}$$

,where the S_P is the selling price of distilled water per litre. Cost of one litre from conventional solar still can be evaluated based on yearly productivity. Market entry of the proposed solar still has been augmented with the payback periods and cost analysis for base system (SSS), solar still with PCM (SSPCM) and solar still with nanoparticles integrated with PCM (SSNPCM). Thus, the payback period of SSNPCM, SSPCM and SSS were found to be 1284, 1159 and 927 days, respectively, as shown in the Table 5.7.

Table 5.7 Estimation of payback period of solar still units

Sl. No.	Type of design	Payback period (days)
1	SSNPCM	1284
2	SSPCM	1159
3	SSS	927

5.6 Market entry of the proposed novel frugal solar still

Our proposed novel frugal solar still (Firm A) enters the market whereas the traditional desalination system (Firm B) to produce distilled water exists in the market. Due to the coexistence of both firms, the market structure would be no longer monopoly and become duopoly in nature.

Let us consider the simple linear demand function as $= a - bQ$; $a, b > 0$, where P is the price and Q is the quantity of water distillate demanded. Under duopoly market scenario, both the firms individually maximize their profit irrespective of the output of another firm.

The profit for firm A (π_A) can be expressed by Eq. 5.13

$$\pi_A = \left(a - b(Q_A + Q_B)\right)Q_A - cQ_A \tag{5.13}$$

,where Q_A and Q_B are the quantity demanded for firms A and B respectively and c is the marginal cost as well as the average cost.

Firm B takes the cost advantage of the government subsidy and produces output at marginal cost and average cost equal to 0. Hence, the profit for firm B (π_B) can be expressed by Eq. 5.14

$$\pi_B = \left(a - b(Q_A + Q_B)\right)Q_B \tag{5.14}$$

On maximizing the profit of firm A (π_A) with respect to Q_A we get Eq. 5.15 from Eq. 5.13.

$$a - 2bQ_A - bQ_B - c = 0 \tag{5.15}$$

Similarly, on maximising the profit of firm B (π_B) with respect to Q_B, we get Eq. 5.16 from Eq. 5.14.

$$a - 2bQ_B - bQ_A = 0 \tag{5.16}$$

On solving Eq. 5.15 and 5.16, we get:

$$Q_A = \frac{a - 2c}{3b}$$

$$Q_B = \frac{a + c}{3b}$$

Hence, total output $= Q_A + Q_B = \frac{2a-c}{3b}$ and, price, $P = \frac{a+c}{3}$

The profits of firm A and B are $\frac{(a-2c)^2}{9b}$ and $\frac{(a+c)^2}{9b}$, respectively.

Hence, the following inferences can be drawn.

(i)   When $a < 2c$, firm A will exit from the market.

(ii)   When $a = 2c$, there will be zero profit for firm A. Then firm A will decide whether to stay or exit from the market.

(iii)   When $a > 2c$, both the firms will sustain and the total output will be the maximum.

(iv)   Firm B will regulate the market dynamics and firm A will only play the residuary role

(v)   The entry of firm B increases the welfare by reducing the market price and increasing the total production under duopoly than that of monopoly. Hence, the scarcity of drinking water in extreme resource limited settings would drastically be reduced with the entry of our novel frugal technology of solar distillation.

5.7 Summary

The proposed solar still rendered the highest output of solar distillate during the summer season due to the augmentation of nanoparticles with PCM stored in copper cylinders. Due to our novel technology, the price of the distilled water from our solar still is quite low (Rs. 3.06/litre) and hence, our solar still has a high potential to be deployed in resource-limited

settings where there is scarcity in portable drinking water. In the scope of our research, the market entry of the solar still through the appropriate economic model has also been developed for its commercialization.